

# The properties of silica aerogels hybridized with SiO<sub>2</sub> nanoparticles by ambient pressure drying

In-Keun Jung<sup>a</sup>, Jyoti L. Gurav<sup>a</sup>, Tae-Jung Ha<sup>a</sup>, Sun Gyu Choi<sup>a</sup>,  
Seungsu Baek<sup>b</sup>, Hyung-Ho Park<sup>a,\*</sup>

<sup>a</sup>Department of Materials Science and Engineering, Yonsei University, Seoul, Republic of Korea

<sup>b</sup>Agency for Defense Development, Daejeon, Republic of Korea

Available online 30 April 2011

## Abstract

In this study, we report the chemical characteristics of silica aerogels that were produced by adding SiO<sub>2</sub> nanoparticles into silica aerogel by ambient pressure drying. We synthesized silica aerogel composites with different weight percentages of SiO<sub>2</sub> nanoparticles ranging from 0 wt% to 0.025 wt% of the total amount of solution. As the wt% of SiO<sub>2</sub> nanoparticles increased, the number of chemical bonds that formed during condensation of the silica aerogel increased because of the presence of surface hydroxyl groups, thus the particle size of the silica aerogels increased. Silica nanoparticle-doping of silica aerogels can be used to control the synthesis of nanocomplex structures.

© 2011 Elsevier Ltd and Techna Group S.r.l. All rights reserved.

**Keywords:** A. Sol–gel processes; B. Composites; C. Thermal properties; D. SiO<sub>2</sub>

## 1. Introduction

Silica aerogels are good thermal insulators because of their extremely low density. Heat transfer in silica aerogels is mediated by solid conductivity, gaseous conductivity, and radiative transmission. Silica aerogels contain an extremely small fraction of solids (1–10%), thus solid conductivity does not contribute significantly to the total thermal conductivity [1]. Additionally, the solids that are present consist of very small particles linked in a three-dimensional network structure with countless ‘dead ends’ [2]. Normally, the particle size of the aerogel determines the microstructural characteristics of the aerogel, such as the specific surface area, pore size, pore distribution, porosity, and so on. These microstructural characteristics strongly affect several properties of aerogels such as their thermal insulation capacity and dielectric constant. The properties of aerogels can be controlled by changing the precursor used or altering the aging time or even drying conditions. However, the properties of aerogels can also be controlled by hybridization with nanoparticles with surface

capping molecules, for example, SiO<sub>2</sub> nanoparticles with hydroxyl groups. Furthermore, by using specific nanoparticles, desired functional properties can be incorporated into the aerogel.

In this paper, we describe the synthesis of silica aerogels incorporating SiO<sub>2</sub> nanoparticles covered with surface hydroxyl groups by a sol–gel process under ambient pressure drying. We characterized the resulting aerogels and studied the overall effects of nanoparticle addition on the chemical properties of the silica aerogels.

## 2. Experimental

Silica aerogels were prepared by hydrolysis and poly condensation of alcohol solvent-diluted alkoxide in the presence of a catalyst [3]. In this study, the precursor was tetraethyl orthosilicate (TEOS), the solvent was methanol, and the catalysts for the hydrolysis and condensation reactions were 0.001 M oxalic acid (C<sub>2</sub>H<sub>2</sub>O<sub>4</sub>, Sigma–Aldrich) and 0.1 M ammonium fluoride (NH<sub>4</sub>F, Sigma–Aldrich), respectively [4]. The catalysts were dissolved in H<sub>2</sub>O. TEOS, methanol, and oxalic acid were mixed together and SiO<sub>2</sub> nanoparticles (Sigma–Aldrich) were added to the solution after the hydrolysis reaction and stirred for 12 h. Various weight percentages (wt%)

\* Corresponding author. Tel.: +82 2 21232853; fax: +82 2 3655882.

E-mail address: [hhpark@yonsei.ac.kr](mailto:hhpark@yonsei.ac.kr) (H.-H. Park).

Table 1

Physical properties of silica aerogels according to SiO<sub>2</sub> nanoparticle content.

	BET surface area (m <sup>2</sup> /g)	Density (g/cm <sup>3</sup> )	Pore size (nm)	Thermal conductivity (W/mK)	Gelation time (min)	Contact angle (°)
0 wt%	531	0.32	23.1	0.075	5	142
0.00625 wt%	672	0.31	18.8	0.082	5	134
0.0125 wt%	772	0.27	19.1	0.078	6	129
0.01875 wt%	542	0.35	20.5	0.081	8	121
0.025 wt%	622	0.35	18.4	0.080	15	129

of SiO<sub>2</sub> nanoparticles were used: 0 wt%, 0.00625 wt%, 0.0125 wt%, 0.01875 wt%, and 0.025 wt%. After stirring, NH<sub>4</sub>F was added to the solution. The volume ratio of the final solution for the SiO<sub>2</sub> aerogels was TEOS::methanol::C<sub>2</sub>H<sub>2</sub>O<sub>4</sub>::NH<sub>4</sub>F = 1::3::0.28::0.1. The final gel was soaked in 1-hexene at 50 °C for 1 day. After solvent exchange, surface modification was carried out with hexamethyldisilazane (HMDZ) for 1 day at 50 °C [5]. The final gel was dried under ambient pressure at 150 °C for 2 h and then at 200 °C for 2 h.

The microstructures of the silica aerogels were investigated by scanning electron microscopy (SEM, JSM-600F, JEOL, Japan). The surface area of the silica aerogel was determined using the Brunauer–Emmitt–Teller (BET, Micromeritics, ASAP 2000, USA) method. Chemical bonds were assessed by Fourier-transform infrared spectroscopy (FT-IR, FTIR-300E, Tokyo, Japan). A contact angle meter was used to confirm the hydrophobicity of the silica aerogels. The thermal stability of the silica aerogel was measured using differential thermal analysis (DTA, TG/DTA-92, Setaram, France), and thermal conductivity was evaluated using a C-T meter (Teleph Company, France).

### 3. Results and discussion

SEM micrographs of the aerogels formed with (a) 0 wt% and (b) 0.025 wt% silica nanoparticles are shown in Fig. 1. The three-dimensional network structures of pure silica aerogel are shown in Fig. 1(a). The particle size of silica aerogels was around 20 nm, as shown in Fig. 1(a). As the wt% of silica nanoparticles increased, the particle size of the silica aerogels increased from 20 nm to 60 nm. Silica nanoparticles contain –OH groups on their surface, which act as nucleation sites for

condensation reactions [6]. As the wt% of silica nanoparticles increased, smaller silica particles agglomerated because of bonding between particles facilitated by the surface –OH groups, which is why the particle size of silica aerogels increased as the wt% of silica particles increased, as shown in Fig. 1(b). The particle size of silica aerogels can therefore be controlled by adding silica nanoparticles without changing the pH, aging time, or drying conditions.

The silica aerogels had a high specific surface area ranging from 531 to 772 m<sup>2</sup>/g. The specific surface area also increased when silica nanoparticles were added; the specific surface area of the silica aerogels doped with nanoparticles ranged from 550 to 690 m<sup>2</sup>/g. The specific surface area increased up to the maximum value of 772 m<sup>2</sup>/g when 0.0125 wt% silica nanoparticles were added. However, at higher wt%, the surface area decreased because of the agglomeration of silica nanoparticles. The overall pore size decreased because micro-pores formed after the addition of silica nanoparticles. During the growth of silica aerogel particles, micro-pores form between the silica nanoparticles [7]. These micro-pores are smaller than the voids that exist in three-dimensional networks of silica aerogels, and provide specific surface area. The density of these micro-pores was similar between the various aerogel samples, as shown in Table 1. Gelation time was effected by the steric effect and the number of –OH groups in solution. A large particle size increases the gelation time – the so-called steric effect [8]. Silica nanoparticles act as nucleation sites for condensation reactions and therefore hinder condensation reactions between silanol particles formed in the hydrolysis reaction [9]. The addition of silica nanoparticles increased the inter-particle distance and therefore the gelation time [10]. The overall pore size decreased because of the formation of micro-pores between the silica nanoparticles. Contact angle measurements of the silica aerogel surfaces revealed that the angle was 142° for the 0 wt% aerogel and 129° for the 0.025 wt% aerogel [11]. Both samples showed hydrophobicity.

The FT-IR spectra given in Fig. 2 show the chemical bonds in silica aerogels that were surface modified with HMDZ. Though silica aerogels are naturally hydrophilic because of the –OH bonds on their surface, we replaced the H of the OH group with the Si–(CH<sub>3</sub>)<sub>3</sub> group. Therefore, –OH bonds were almost completely absent from the spectra. The hydrophobicity of the silica aerogels was therefore most likely due to moisture absorption from the air, because there was no absorption peak at 3300 cm<sup>–1</sup> from –OH bonds [12]. The peaks near 1100 cm<sup>–1</sup>, 800 cm<sup>–1</sup>, and 470 cm<sup>–1</sup> are Si–O–Si bonding peaks [13]. The

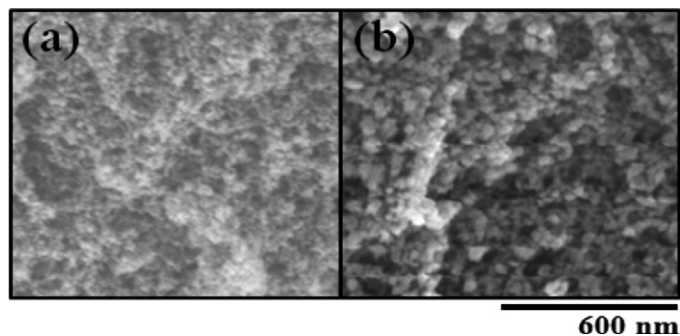


Fig. 1. SEM planar image of a SiO<sub>2</sub> aerogel: (a) with 0 wt% and (b) with 0.025 wt% silica nanoparticles.

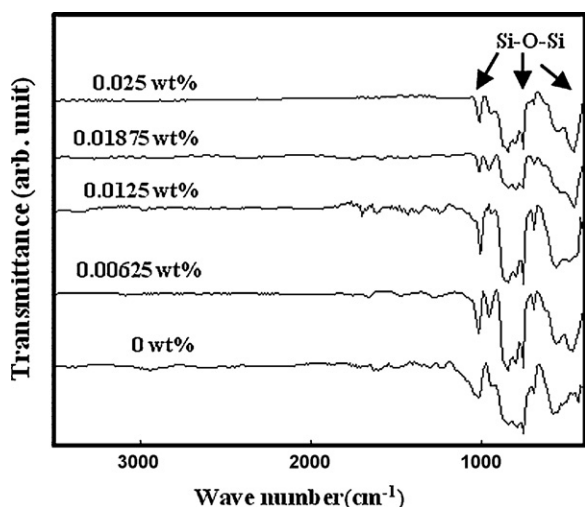


Fig. 2. FT-IR spectra of silica aerogel hybridized silica nanoparticles dried under ambient pressure.

Si–O–Si peak at  $1100\text{ cm}^{-1}$  corresponds to an asymmetric bond and the  $800\text{ cm}^{-1}$  peak corresponds to a symmetric bond. The  $850\text{ cm}^{-1}$  and  $1255\text{ cm}^{-1}$  peaks indicate  $-\text{CH}_3$  bonds contributed by  $\text{Si}(\text{CH}_3)_3$  [14].

Fig. 3 shows FT-IR spectra for silica aerogels doped with silica nanoparticles and then heated at  $700^\circ\text{C}$  for 2 h. The  $-\text{OH}$  groups arose due to oxidation of  $-\text{CH}_3$  groups. This change was much more noticeable in the 0.025 wt% sample than the 0 wt% sample. The OH peak ( $3300\text{ cm}^{-1}$ ) of the 0.025 wt% sample is bigger and wider than that of the 0 wt% sample, because of the presence of silica nanoparticles in the 0.025 wt% sample. The DTA curve of an ambient pressure-dried silica aerogel that was surface modified is shown in Fig. 4. We attributed the exothermic peaks at 365 and  $369^\circ\text{C}$  to oxidation of  $-\text{CH}_3$  because of the surface modification process and the presence of residual organics ( $-\text{OC}_2\text{H}_5$ ). These results indicate that silica aerogels with added silica nanoparticles were hydrophobic at temperatures of  $365^\circ\text{C}$  and  $369^\circ\text{C}$ . However, silica aerogels showed hydrophilic behavior when the silica aerogels were heated to temperatures greater than  $365^\circ\text{C}$  and  $369^\circ\text{C}$  because

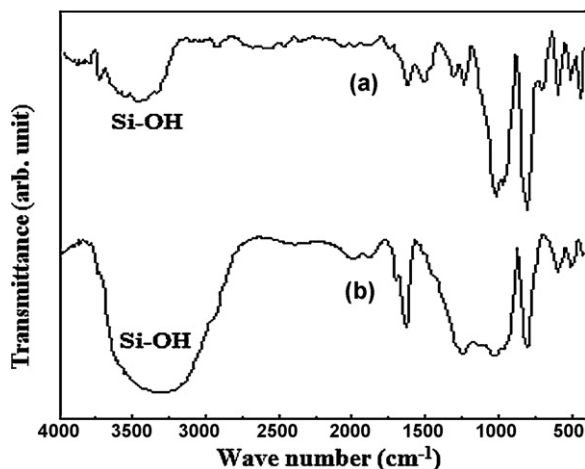


Fig. 3. FT-IR spectra of silica aerogels doped with (a) 0 wt% and (b) 0.025 wt% silica nanoparticles after heating at  $700^\circ\text{C}$  for 2 h.

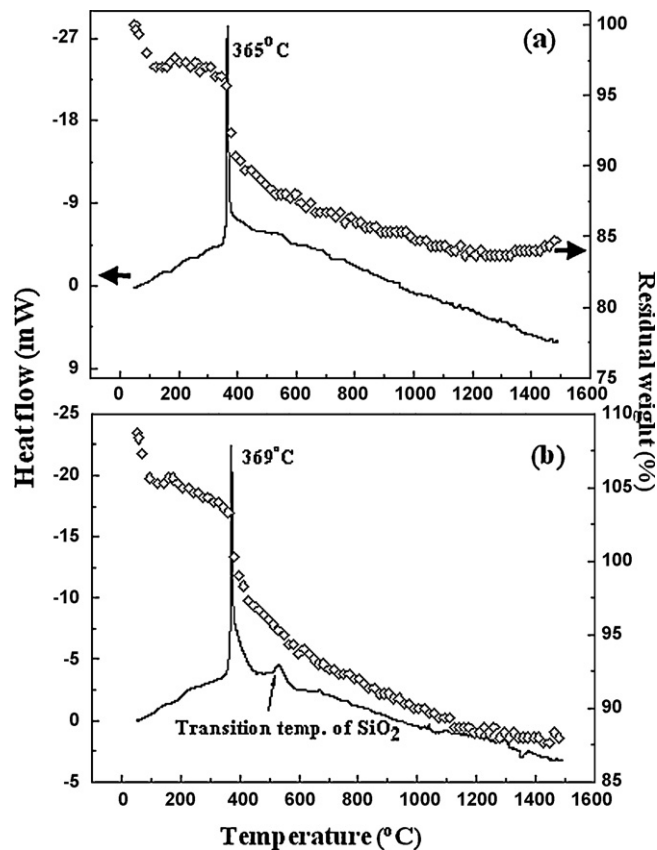


Fig. 4. DTA curve of silica aerogels doped with (a) 0 wt% and (b) 0.025 wt% silica nanoparticles.

of oxidation of surface  $-\text{CH}_3$  groups [15]. The  $-\text{OH}$  groups formed as a result of the oxidation of  $-\text{CH}_3$ . These  $-\text{OH}$  groups then reacted with other Si–OH groups to produce  $\text{H}_2\text{O}$ , which was lost to the atmosphere by evaporation.

The curve of the 0.025 wt% sample had the same transition temperature as fused glass, because of the presence of silica nanoparticles. The 0 wt% sample did not show the transition temperature of glass even though the samples had the same chemical composition. This phenomenon can be explained by the difference in bonding types between silica nanoparticles and silica aerogels.

The thermal conductivities of the silica aerogel samples are shown in Table 1. Silica nanoparticles were added to the silica aerogel and partially aggregated or behaved as nucleation sites. Pure silica aerogel showed the lowest thermal conductivity. As the wt% of silica nanoparticles increased, the thermal conductivity of the aerogels also increased slightly. This is because the increase in the density of aerogels due to the addition of silica nanoparticles induced a decrease in porosity, hence thermal conduction through the solid portion of the samples increased [16].

#### 4. Conclusions

We investigated the effects of silica nanoparticle addition to silica aerogels on the chemical and material properties of the resultant aerogels. As the wt% of  $\text{SiO}_2$  nanoparticles increased,

density and thermal conductivity increased due to an increase in the solid percentage of the sample, and hence porosity decreased. Overall thermal conductivity and density remained the same. Pure silica aerogel and SiO<sub>2</sub> nanoparticle-doped aerogels showed hydrophobicity. After addition of SiO<sub>2</sub> nanoparticles, the particle size of the aerogels increased from 20 nm to 60 nm. The surface area of the aerogel samples increased as the amount of silica nanoparticles added increased. Our results indicate that the introduction of silica nanoparticles with surface hydroxyl groups into silica sol is a feasible way to control the synthesis of nanocomplex structures.

## Acknowledgements

This work was supported by a grant from DAPA and ADD, Republic of Korea. This work was also supported by the Second Stage of Brain Korea 21 Project in 2010. Experiments at PLS were supported in part by MEST and POSTECH.

## References

- [1] J.L. Gurav, D.Y. Nadargi, A.V. Rao, Effect of mixed catalysts system on TEOS-based silica aerogels dried at ambient pressure, *Applied Surface Science* 255 (2008) 3019–3027.
- [2] S. Alexander, Vibrations of fractals and scattering of light from aerogels, *Physical Review B* 40 (1989) 7953–7965.
- [3] A.V. Rao, S.D. Bhagat, Synthesis and physical properties of TEOS-based silica aerogels prepared by two step (acid–base) sol–gel process, *Solid State Sciences* 6 (2004) 945–952.
- [4] J. Mrowiec-Białoń, L. Pająk, A.B. Jarzębski, A.I. Lachowski, J.J. Malinowski, Morphology of silica aerogels obtained from the process catalyzed by NH<sub>4</sub>F and NH<sub>4</sub>OH, *Langmuir* 13 (1997) 6310–6314.
- [5] A.P. Rao, A.V. Rao, G.M. Pajonk, Hydrophobic and physical properties of the ambient pressure dried silica aerogels with sodium silicate precursor using various surface modification agents, *Applied Surface Science* 253 (2007) 6032–6040.
- [6] K. Zhang, J. Ma, B. Zhang, S. Zhao, Y. Li, Y. Xu, W. Yu, J. Wang, Synthesis of thermoresponsive silica nanoparticle/PNIPAM hybrids by aqueous surface-initiated atom transfer radical polymerization, *Materials Letters* 61 (2007) 949–952.
- [7] S.D. Bhagat, Y.H. Kim, Y.S. Ahn, J.G. Yeo, Textural properties of ambient pressure dried water-glass based silica aerogel beads: one day synthesis, *Microporous and Mesoporous Materials* 96 (2006) 237–244.
- [8] T. Woignier, J. Phalippou, M. Prassas, Glasses from aerogels, *Journal of Materials Science* 25 (1990) 3118–3126.
- [9] C.T. Wang, C.L. Wu, I.-H. Chen, Y.H. Huang, Humidity sensors based on silica nanoparticle aerogel thin films, *Sensors and Actuators B* 107 (2005) 402–410.
- [10] L. Boogh, B. Pettersson, J.E. Månson, Dendritic hyperbranched polymers as tougheners for epoxy resins, *Polymer* 40 (1999) 2249–2261.
- [11] A.V. Rao, M.M. Kulkarni, Hydrophobic properties of TMOS/TMES-based silica aerogels, *Materials Research Bulletin* 37 (2002) 1667–1677.
- [12] P.R. Aravind, P. Mukundan, P. Krishna Pillai, K.G.K. Warriar, Mesoporous silica–alumina aerogels with high thermal pore stability through hybrid sol–gel route followed by subcritical drying, *Microporous and Mesoporous Materials* 96 (2006) 14–20.
- [13] C.J. Lee, G.S. Kim, S.H. Hyun, Synthesis of silica aerogels from water-glass via new modified ambient drying, *Journal of Materials Science* 37 (2002) 2237–2241.
- [14] H.-S. Yang, S.-Y. Choi, S.-H. Hyun, H.-H. Park, J.-K. Hong, Ambient dried low dielectric SiO<sub>2</sub> aerogel thin film, *Journal of Non-Crystalline Solids* 221 (1997) 151–156.
- [15] S. Cao, K.L. Yeung, P.-L. Yue, Preparation of freestanding and crack-free titania–silica aerogels and their performance for gas phase, photocatalytic oxidation of VOCs, *Applied Catalysis B: Environmental* 68 (2006) 99–108.
- [16] M.-A. Einarsrud, S. Hæreid, V. Wittwer, Some thermal and optical properties of a new transparent silica aerogel material with low density, *Solar Energy Materials and Solar Cells* 31 (1993) 341–347.